Advanced Materials Science and Technology; 2020;2:2
www.omniscient.sg

Original Research

Open Access

Omniscient Pte.Ltd.

Investigation on the Pulsed TIG Welding of Nickel-Base Alloy for Improved Microstructure and Weld Penetration

Dayou Pan*, Yijun Man

Singapore Institute of Manufacturing Technology, 73 Nanyang Drive, Singapore 637662

***corresponding e-mail:** dypan@simtech.a-star.edu.sg

Abstract

In this study, a novel pulsed tungsten inert gas (TIG) welding technique that is capable of effectively improving the weldabilities of nickel-based alloys was developed. The correlation between process parameters and material properties was studied. The effects of ratios of pulse to background welding currents on hardness and penetration in welds and heat-affected zones (HAZs) of Inconel 718 alloy were investigated experimentally by using the pulsed TIG welding technique. It is found that with an increasing ratio of the pulse to background welding current, the hardness in welds increased from 2% to 3.5%, compared to that in constant current TIG welding at the same level of heat input. When the ratio of pulse to background welding current is higher than 6, the penetration in weld was improved significantly by up to 61%. Research work has demonstrated that the pulsed TIG welding technique is an effective approach to control the microstructure and reduce cracking susceptibilities.

Keywords

TIG welding; GTAW; Pulsation; Weld penetration; Arc physics.

1. INTRODUCTION

Electric arc is an effective heat source that used to heat and melt the work-pieces to be welded in arc welding processes. As one of the arc welding processes, tungsten inert gas (TIG) welding or gas tungsten arc welding (GTAW) has been extensively used in producing high integrity Ni-based alloy joints that can be applied in harsh environment, such as high temperature, high pressure, high corrosion & erosion etc. The productivity of the TIG welding, however, is relatively lower compared to other arc welding processes such as manual metal arc (MMA) welding, metal inert gas (MIG) welding, and submerged arc welding (SAW) because of its tungsten electrode's

limited current-carrying capacity. Over the past half a century, researchers have kept in investigating, developing, and optimizing various TIG welding techniques, in order to improve the TIG welding productivity, and the weldabilities for those high performance, but difficult-to-weld metals and alloys. The main approaches are to increase TIG welding travel speed without increasing welding current, and to improve the properties of the welded joints by the refinement of grain size for those heat-resistant metals and alloys. [1-7]

Various pulsed TIG welding techniques have been successfully developed for industrial applications. It has been demonstrated that the pulsed TIG welding with higher pulsation frequency is capable of making the TIG welding arc more rigid and directional, which leads to more effective thermal transfer between the welding arc and the work-pieces to be welded, and eventually leads to increase in welding productivity in terms of weld penetration and/or welding travel speed. [5-9]

Similar to the pulsation frequency of the TIG welding current, the ratio of pulse to background welding current is another process parameter that required to be investigated. There are not many investigations on the effect of the ratio of pulse to background welding current [5]. For a given average welding current in the pulsed TIG welding process, there will be various combinations of pulse to background welding current. Therefore, it is worth investigating the ratio of pulse to background current in the pulsed TIG welding, so as to identify how the ratio of pulse to background welding current affect the interaction between the TIG welding arc and the molten welding pool as well as the characteristics of the welded joints. [1, 5].

2. MATERIALS AND METHODS

2.1. Materials

As the most widely applied nickel-based alloys, Inconel 625 and Inconel 718 alloy sheets with dimensions of 3.2mm (T) x 40mm (W) x 80mm (L) were used as the work-pieces or base metals.

2.2. Welding Experiment Procedure

Miller Dynasty 350 inverter welding power source was employed to perform the welding trials. A tungsten electrode (specification: AWS EWCe-2) with diameter at 2.4 mm was used in the TIG welding torch. A welding fixture that is capable of providing back shielding for the welding coupon was applied. During welding, the previously tack-welded welding coupon was firmly clamped onto the welding fixture, and the TIG welding torch was mounted on a motorized linear travel carriage to perform mechanized welding. The welding experiment set-up is shown in Figure 1. For all the welding experiments, the arc length or the distance between the tungsten electrode tip and the work-piece was set at 2.4 mm, and the welding travel speed was set at 120 mm/min. Square butt joint was applied. The length of the weld seam was at around 80mm. The Ar gas flow-rates for both top and back shielding were set at 16 l/min. and 10 l/min, respectively. Figure 2 illustrates the relative positions between the TIG welding torch and the work-pieces or base metals, as well as the configuration of the welding joint.

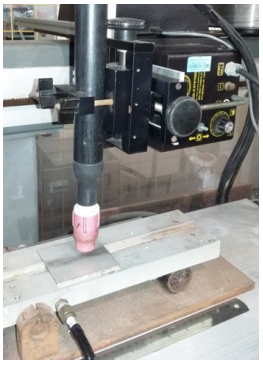

Fig. 1 Set-up of welding experiment

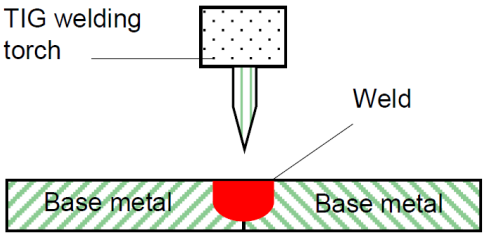

Fig. 2 Illustration of relative positions between the TIG welding torch and the base metals, as well as the configuration of the welding joint

2.3. Pulsation of TIG Welding Current

The welding power source can be used for the TIG welding not only in the constant current mode but also in the pulsed current mode (i.e., pulsed TIG welding). Figure 3 shows a typical waveform of a pulsed TIG welding current.

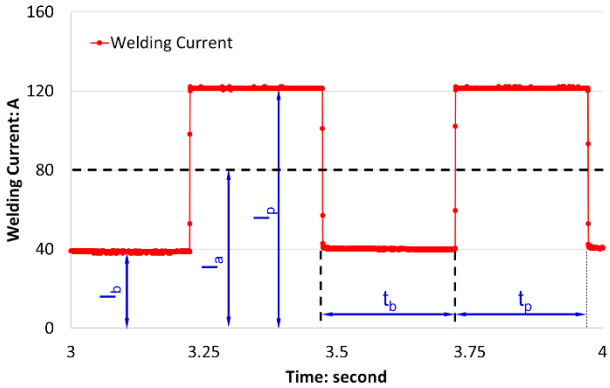

Fig. 3 A typical waveform of the pulsed TIG welding current

where:

I_p denotes pulse welding current (A);

I_b denotes background welding current (A);

I_a denotes average welding current (A);

t_p denotes time duration at pulse welding current (s);

t_b denotes time duration at background welding current (s).

Mathematically the frequency (f) of the pulsed TIG welding current and the average welding current (I_a), can be worked out via Equations (1) and (2) below, respectively.

$$f = \frac{1}{t_p + t_b} \tag{1}$$

$$I_a = \frac{(I_p \times t_p) + (I_b \times t_b)}{t_p + t_b} \tag{2}$$

2.4. Welding Heat Input

Welding heat input is an important indicator that related to the properties of the welded joint, which effectively represents the amount of heat (or energy) that is required to apply to a unit length of a weld, so as to achieve satisfactory properties in the whole welded joint [10]. The welding heat input can be mathematically expressed as in Equation 3, as long as the actual values for welding current, welding voltage, and welding travel speed are captured and recorded [10].

$$Heat\ Input\left(J/mm\right)=\frac{Welding\ Current\left(A\right)\times Welding\ Voltage\left(V\right)\times 60}{Welding\ Travel\ Speed\left(mm/\min.\right)} \quad (3)$$

2.5. Welding Experiment Matrix

A lower pulsation frequency (f) at 1Hz merely was selected, in order to limit the effect of the pulsation frequency (f) to the lowest level, and to clearly reveal the effect of the ratio of pulse to background welding current. For a given I_a value in the pulsed TIG welding process, there are unlimited combinations of I_p and I_b. To explore how the ratio of pulse to background welding current influence the characteristics of the welded joints, the primary focus was put on the values of I_p, while maintaining I_b to be at the lowest possible level based on the steadiness of I_b. A couple of such combinations of I_p and I_b were chosen, while trying to maintain I_a value at 100A or very close to 100A. Accordingly, t_p and t_b were set at different levels. The details of the pulsed TIG welding process set up are tabulated in Table 1.

Table 1. The details of the programed welding parameters used in the trials

Programed ratio of I_p to I_b	Programed ratio of t_p to t_b	Average welding current $(I_a)^*$, A	Background welding current $(I_b)^*$, A
100A – 100A	N.A.	100	N.A.
120A – 20A	0.8s – 0.2s	100	20.4 (17% of I_p)
135A – 20A	0.7s – 0.3s	100.5	20.25 (15% of I_p)
150A – 20A	0.6s – 0.4s	98	19.5 (13% of I_p)
180A – 20A	0.5s – 0.5s	100	19.8 (11% of I_p)
220A – 20A	0.4s – 0.6s	100	19.8 (9% of I_p)
285A – 20A	0.3s – 0.7s	99.5	19.95 (7% of I_p)

*: the values are calculated from the programed values.

2.6. Actual Values of the Welding Process Parameters

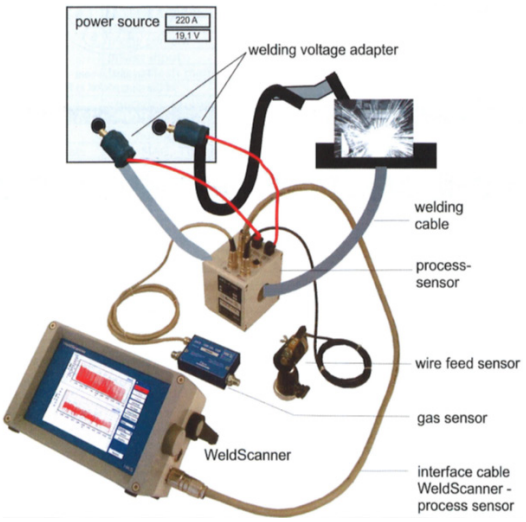

Fig. 4 A welding DAQ device employed to capture and record welding parameters

In almost all the arc welding operations, more or less, there are differences between the programed parameter values and the actual parameter values, this is because the actual parameter values are typically measured by additional devices that are calibrated. In addition, the nature of this study is highly relevant to the physics or characteristics of the electric arc. For these reasons, a commercially available welding data acquisition (DAQ) device, as shown in Figure 4, was applied to accurately capture and record the actual welding process parameters. The calibrated DAQ device was made by HKS-Prozesstechnik GmbH, which is capable of capturing and recording

both welding current and welding voltage values with sampling rate at up to 3000Hz. With such a high sampling rate, this welding DAQ device is capable of precisely capturing all the features and details of the welding process parameter signals such as welding current and welding voltage [7].

3. RESULTS AND DISSCUSSIONS

3.1. Actual Welding Process Parameters Captured and Recorded

By using the calibrated welding DAQ device, the details of the welding process parameters for all the welding trials listed in the experiment matrix were captured and recorded, which is tabulated in Table 2 below. In addition, the actual welding heat inputs for all the trials were calculated and tabulated below as well.

Table 2. The details of the welding process parameter values recorded and calculated

Ratio* of Ip to I_b	Ratio* of t_p to t_b	Average welding current (I_a)**, A	Back-ground welding current (I_b)**, A	Average welding current (I_a)***, A	Average welding voltage (V_a)***, V	Welding travel speed, mm/min.	Actual heat input, J/mm
100A – 100A	N.A.	100	N.A.	103.9	14.68	120	762.63
120A – 20A	0.8s – 0.2s	100	20.4 (17% of I_p)	104.1	14.56	120	758.35
135A – 20A	0.7s – 0.3s	100.5	20.25 (15% of I_p)	104.53	14.42	120	753.63
150A – 20A	0.6s – 0.4s	98	19.5 (13% of I_p)	101.5	13.99	120	710.06
180A – 20A	0.5s – 0.5s	100	19.8 (11% of I_p)	104.0	13.98	120	726.83
220A – 20A	0.4s – 0.6s	100	19.8 (9% of I_p)	103.7	13.64	120	707.38
285A – 20A	0.3s – 0.7s	99.5	19.95 (7% of I_p)	103.0	12.83	120	661.19

*: the values are programed;
**: the values are calculated from the programed values;
***: the values are captured by the welding DAQ device

3.2. Correlations among the Average Welding Current, the Average Welding Voltage, and the Actual Heat Input

Figure 5 shows a typical captured waveform with a ratio of pulse to background welding current at 120A – 20A. According to Table 2, the correlations among the actual welding current, actual welding voltage, and actual welding heat input, at various ratios of pulse to background welding current, were plotted in Figures 6 and 7, respectively. Figure 6 shows the correlation between I_a and the average welding voltage (V_a) at various ratios of pulse to background welding current. It can be seen that with increase in the ratio, the actual I_a generally keeps unchanged, while V_a starts to decrease gradually, from 14.5V down to 12.8V, without any exception. This could be ascribed to the change in the characteristics of the TIG welding arc. As an electric arc used in welding operation, it transfers heat to the work-piece, in addition, it also exerts force or pressure to the work-piece. To maintain such an electrical arc, however, the energy required should be a constant, as long as the average welding current remains unchanged. The decrease in the average welding voltage could be caused by the increase in the electric arc force or pressure exerted to the molten pool on the work-pieces to be welded [11]. This will be discussed in detail in the subsequent section. There is a slight drop (at around 3%) in I_a while the ratio was at 150A – 20A. This could be ascribed to the system error caused by welding power source itself, as the 20A of background welding current had to be set at 150A X 13%, which was at 19.5A, rather than exactly 20A. In addition, I_a calculated by the programed value was at 98A rather than 100A, which led to the relatively lower average welding current at 101.5A compared with the others, consequently it causes the lower heat input to the weld at this ratio. As can be seen in Figure 7, there is a drop in heat input at ratio of 150A – 20A, which is ascribed to the lower welding current (at 101.5A, around 3% lower than the others) at this ratio. Also, the actual heat input starts to decrease quickly, from lower ratio to higher ratio up to 285A – 20A. This is attributed to the decrease in V_a.

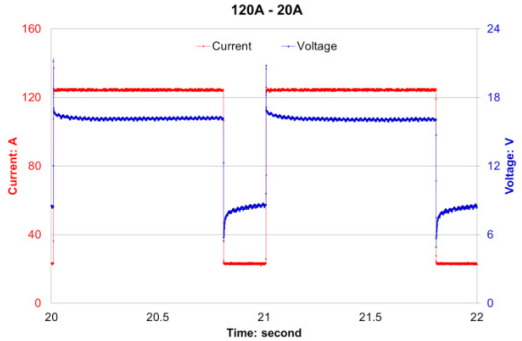

Fig. 5 Actual waveform of welding current and welding voltage at ratio of 120A – 20A.

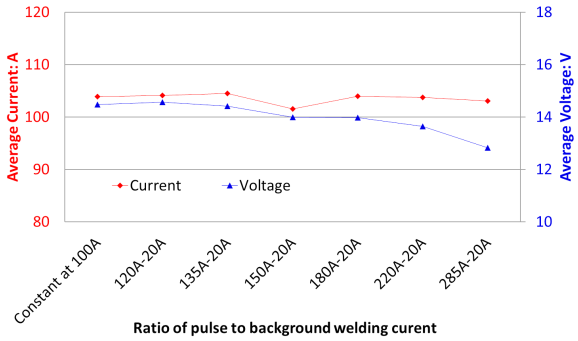

Fig. 6 Correlation between the average welding current (I_a) and the average welding voltage (V_a) at various ratios of pulse to background welding current.

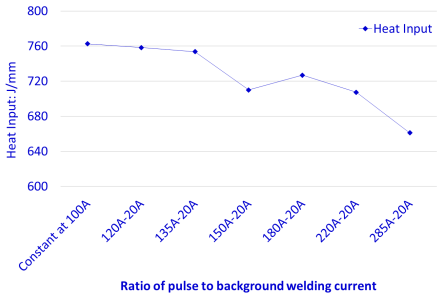

Fig. 7 Correlation between the actual heat input, at various ratios of pulse to background welding current.

3.3. Effect of Ratio of Pulse to Background Current on Penetration in the Weld and Microstructure

In the experiment trials, the welded Inconel 718 coupons were one-pass welded on butt joint configuration, as shown in Figure 8. To explore this effect, the depth of the weld protrusion below the back surface of the welding coupon (base metals) was used to evaluate the penetration in the weld. Figure 9 shows macro-and micro-structures of the welded joints made at various ratios.

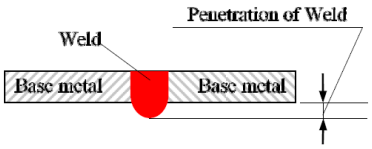

Fig. 8 Illustration of weld penetration for a one-pass welded on butt joint configuration.

The macro-structures of all the welding samples reveal that all the welds are fully penetrated, and free from any welding defect. The micro-structures of all the welded joints can be characterized as fine dendrite structures,

which indicating all the welded joints have sound mechanical and metallurgical properties. It should be pointed out that, the ripples in both weld sides close to the base metals could be the evidence of vibration in the molten pools during the pulsed TIG welding process. It can be clearly seen in Figure 9 that with increase in pulse welding current value, the amount of the ripple increases in weld accordingly, i.e. more vibrations generated in weld. Therefore, the higher ratio of pulse to background welding current could contribute to the vibration in weld, consequently refine the grain size in weld during solidification. This will be discussed in the subsequent section.

To explore the effect of ratio of pulse to background welding current on weld penetration, the penetrations of welds made at various ratios of pulse to background welding current were measured and shown in Table 3. The correlation between the ratios of pulse to background welding current and the weld penetrations is plotted, which is shown in Figure 10. As can be seen from Figure 10, in the range of from 120A – 20A to 180A – 20A, the weld penetrations are generally quite close. However, starting from 180A – 20A, up to 285A – 20A, the weld penetrations increase significantly. The significant increase in weld penetration at higher ratio has nothing to do with the welding voltage and the heat input. This is because it has been verified that with the increase in the ratio or pulse welding value, the welding voltage and the heat input tend to decrease (refer to Figure 7). According to [11], the correlation between the welding current and the welding arc force can be expressed as:

$$F = \frac{\mu_0 I^2}{8\pi}\left(2ln\frac{R_2}{R_1}+1\right) \tag{4}$$

where:

F denotes the integrated arc force, in N;

μ_0 denotes permeability in free space, in henry/m;

denotes welding current, in A;

R_1 and R_2 denote radius of the arc at the cathode and anode regions respectively, in meter.

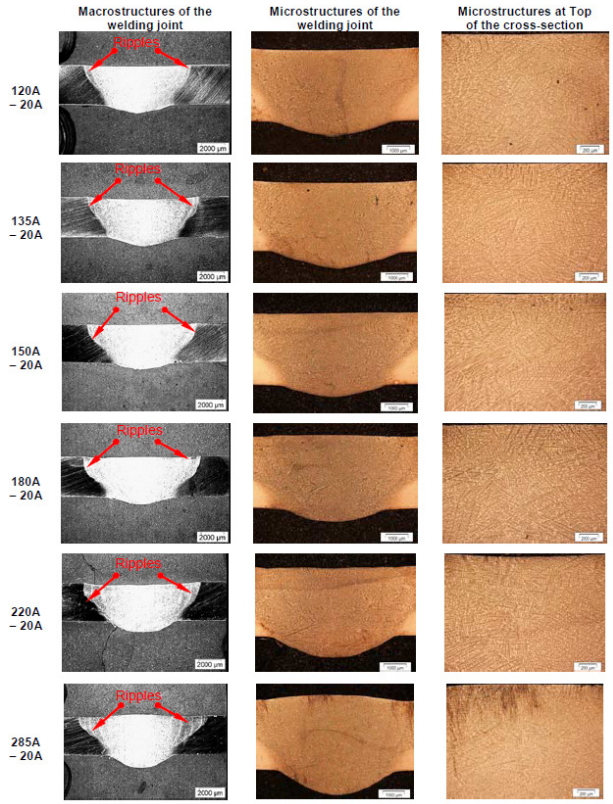

Fig. 9 Macro- and microstructures of the welded Inconel 718 joints made at various ratios.

Table 3 Penetrations of welds made at various ratios of pulse to background welding current

Ratio* of I_p to I_b	Ratio* of t_p to t_b	Average welding current (I_a)**, A	Average welding current (I_a)***, A	Average welding voltage (V_a)***, V	Actual heat input, J/mm	Weld penetration, mm
100 (constant)	N.A.	100	103.9	14.68	762.63	N.A. (Note 1)
120A – 20A	0.8s – 0.2s	100	104.1	14.56	758.35	0.703
135A – 20A	0.7s – 0.3s	100.5	104.5	14.42	753.63	0.726
150A – 20A	0.6s – 0.4s	98	101.5	13.99	710.06	0.635 (Note 2)
180A – 20A	0.5s – 0.5s	100	104.0	13.98	726.83	0.726
220A – 20A	0.4s – 0.6s	100	103.7	13.64	707.38	0.953
285A – 20A	0.3s – 0.7s	99.5	103.0	12.83	661.19	1.134

***Note 1*:**

It was found out in the welding trials in this investigation that the width of the weld seam welded with 100A of constant current is inconsistent, compared to that welded with pulsed welding current. Typically, the width of the seam welded with constant welding current is narrower in the starting point, and is wider in the ending point. Thus, the penetration of the seam welded with the constant welding current could be inconsistent as well.

***Note 2*:**

In addition, the lower value in the weld penetration at ratio of 150A – 20A was caused by the lower average welding current and heat input as well.

***Note 3*:**

*: *the values are programed*;

**: *the values are calculated from the programed values*;

***: *the values are captured by the welding DAQ device*.

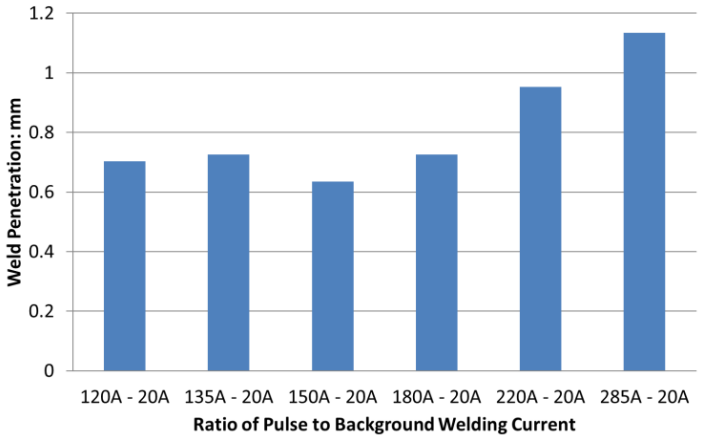

Fig. 10 Correlation between the ratio of pulse to background welding current and weld penetration.

Therefore, the welding current or I_p plays critical role in the welding arc force (F), which results in significant impact or vibration on the molten pool. The increase in weld penetration might have something to do with the force (F) generated by the electric arc (refer to Equation 4). Because of the increase in I_p, the arc force (F) increases significantly based on the value of I_p^2. Therefore, the higher the Ip, the higher the arc force (F). To explain why the weld penetrations are quite close when the ratios are at 120A – 20A, 135A – 20A, 150A – 20A, the reasons could be (1) the I_p is not high enough when the ratios are at 120A – 20A and 135A – 20A, i.e. the arc force is not strong enough to enhance the weld penetration; (2) the actual average welding current at the ratio of 150A – 20A is at 101.5A only (Refer to Table 3), even lower than that at ratios of 120A – 20A and 135A - 20A, consequently the weld penetration is slightly lower. The increase in arc force (F) could change an outward directed flow in the molten pool into a downward directed flow, consequently increase the weld penetration [1]. Figure 11 illustrates the outward directed and downward directed flows. Therefore, increasing I_p in the pulsed TIG welding is an effective way to improve the productivity for welding nickel-based alloys or other stainless steels, in terms of increase in weld penetration.

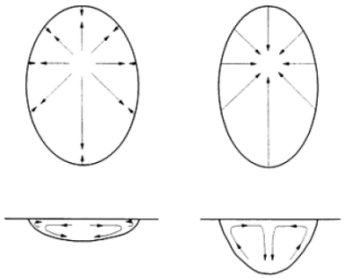

Fig. 11 Illustration of an outward directed (left) and a downward directed (right) flows [1].

3.4. Effect of Ratio of Pulse to Background Welding Current on Hardness and Grain Refinement

Vickers hardness test was carried out to evaluate how the ratio of pulse to background current influence the hardness values in welds and HAZs. For the Vickers hardness tests, a line of indentations which crossed weld, HAZs, and base metals, with 1mm of spacing between any adjoining two indentations, was made at 300g of loading force. The indentation line was set to be parallel to the top surface of the hardness specimen, and around 1mm below to the top surface, which is illustrated in Figure 12.

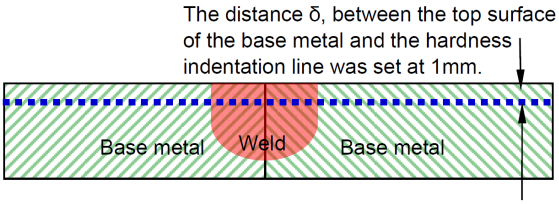

Fig. 12 Illustration of location of the indentation line in the welding specimen.

Over 20 indentations were made in each line, and there were around 10 indentations that cross the region covering the weld and HAZs. Figure 13 shows the distribution of the hardness in the weld, HAZs, and base metals. It can be seen clearly that, without any exception, for all the welding coupons welded with various ratios of pulse to background welding current, the hardness values in the weld and HAZs are generally higher, i.e., for the welding coupon made with constant welding current at 100A, the hardness values in the weld and HAZs are generally lower.

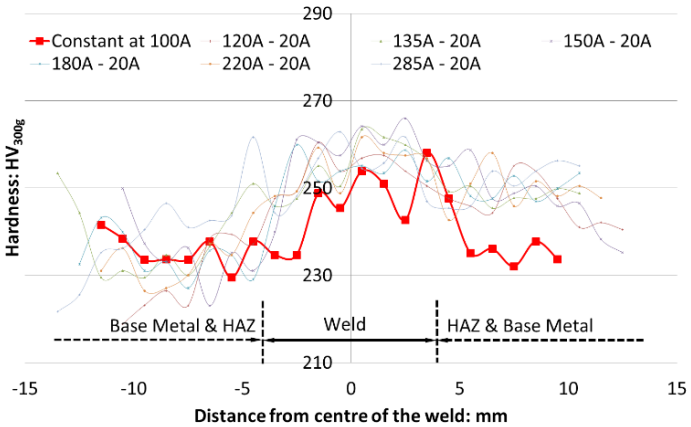

Fig. 13 Hardness distributions in weld, HAZs, and base metals for welding samples welded at various ratios of pulse to background welding currents, as well as constant welding current at 100A.

To clearly reveal how the ratio of pulse to background welding current influences hardness values in weld and HAZs, the average hardness values of the 10 indentations crossing the weld and HAZs for each line were worked out. The average hardness values at various ratios were plotted and shown in Figure 14.

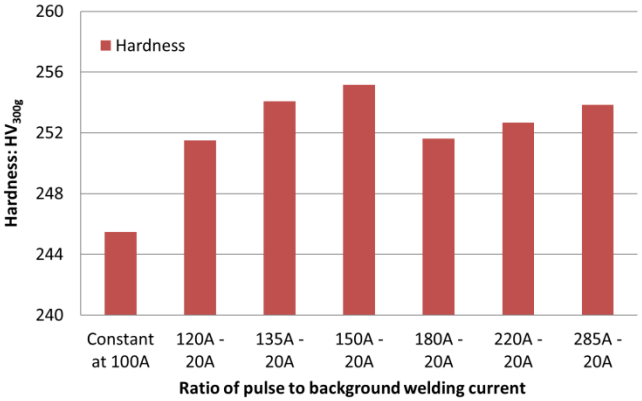

Fig. 14 Correlation between ratios of pulse to background welding current and hardness in weld and HAZs.

It can be seen clearly from Figure 14, that with the lower pulsation at 1Hz merely, various ratios of pulse to background welding current play a role in increasing hardness values in the weld and HAZs. The increase in the hardness values ranges from 2% to 3.5%, compared to the welding sample made with the constant welding current at 100A. However, it should be pointed out that the hardness values of the samples welded at various ratios of pulse to background welding current are quite close, ranging from HV_{300g} 251 to HV_{300g} 255 merely, but obviously higher than that made with the constant welding current at 100A, which is HV_{300g} 245. The working mechanism for hardness increase in the weld and HAZs could be ascribed to following factors:

- The higher I_p exerts high force or pressure on the molten pool, which leads to strong impact or vibration on the weld, consequently increases the weld hardness via grain size refinement [10];
- With increase in I_p, while the background welding current remains unchanged and at the lowest possible value, the heat input to the weld decreases due to the decrease in welding voltage (refer to Table 2, and Figures 6 and 7), which leads to higher cooling rate during the solidification of the welding pool, consequently refines the grain size;
- It should be also pointed out that the welding coupon made with the ratio of 150A – 20A has the highest hardness value. This indicates that the higher hardness value is caused by the higher cooling rate during the solidification of the welding pool. This is because the welding coupon made with the ratio of 150A – 20A has the lower I_a and/or lower heat input.

Figure 15 shows microstructures of the welded joints welded with the constant welding current at 100A and with the ratio of pulse to background welding current at 285A – 20A, respectively. It seems the grain size refinement in the welded joint made with ratio of pulse to background welding current at 285A – 20A cannot be visualized readily. This result has good agreement with that shown in the Ref. 5. This could be the reason of the slight increase in the hardness value, which is up to 3.5% merely.

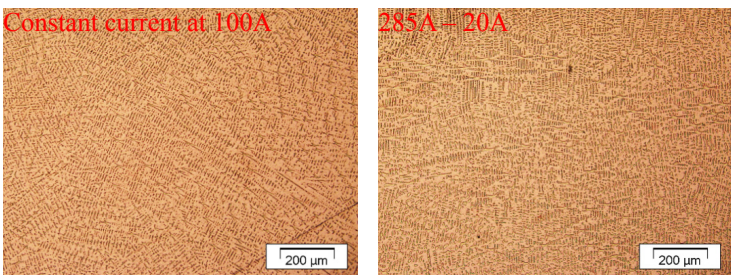

Fig. 15 Microstructures of the Inconel 718 welded joints made with constant welding current at 100A and with ratio of pulse to background welding current at 285A – 20A, respectively.

As a comparison of effect on grain size refinement in different nickel-based alloy base metals, both Inconel 625 and 718 alloys were welded at the same level of welding current (constant at 50A), with the same welding experiment set-up mentioned in Section 2.2. Figure 16 shows the microstructures in the Inconel 625 and 718 alloy welded joints. It can be seen clearly that there are coarsened grains in the HAZ of the Inconel 625 welded joint, while the coarsened grains in the Inconel 718 alloy welded joint are not obvious. This could be ascribed to the difference in the thermal conductivity of the nickel-based alloys [12]. Inconel 625 alloy is a Ni-Cr-Mo alloy with less than 5% of Fe content, while Inconel 718 is a Ni-Cr-Fe alloy with up to 20% of Fe content. The high Fe content in Inconel 718 could be the good thermal conductor, which reduces the tendency of the grain size coarsening during welding [12]. This could be the another reason that the correlation between the hardness increase and grain size refinement in the Inconel 718 alloy joints made with the pulsed TIG welding process cannot be visualized clearly in this study. Therefore, increasing I_p in the pulsed TIG welding is a very simple approach to improve the weldability for welding nickel-based alloys or other stainless steels, in terms of grain size refinement.

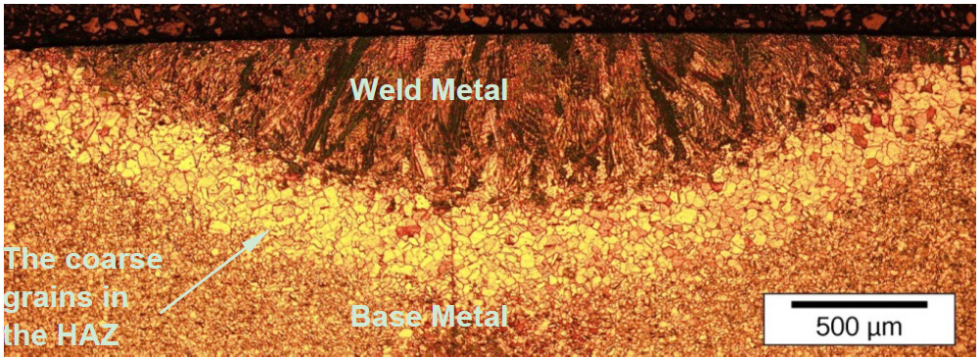

Inconel 625 weld

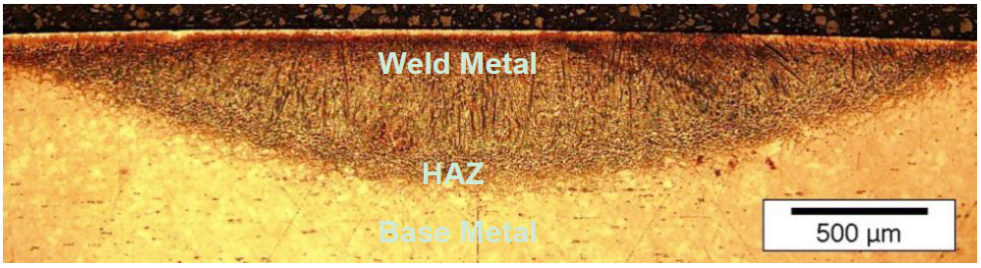

Inconel 718 weld

Fig. 16 Comparison of macrostructures of Inconel 625 alloy and Inconel 718 alloy welds made at 50A, respectively.

4. CONCLUSIONS

The pulsed TIG welding of nickel-based alloys with various ratios of pulse to background welding current were carried out. The correlations among the average welding current, the average welding voltage, and the actual heat input were identified. The effects of the ratio of pulse to background welding current on weld penetration, hardness and microstructure and were studied and analyzed. The conclusions can be drawn as follows:

● In the pulsed TIG welding even with lower pulsation frequency (f) at 1Hz merely, the ratio of the pulse to background welding current changes the characteristics of the TIG welding arc. With the increase in the ratio, the welding arc tends to be thermally weaker in terms of the decrease in the welding voltage or the heat input to the work-pieces to be welded, and mechanically stronger in terms of the increase in the welding arc force that exerted to the molten pool on the work-pieces to be welded;

● The pulse TIG welding technique developed in the study can significantly improve the weld penetration and weldability for nickel-based alloys. It is found that the higher ratio of the pulse to background welding current is

capable of producing weld with deeper penetration even the average welding current (I_a) remains unchanged. Up to 61% increase of penetration has been achieved in this study;

● The welding current or the pulse welding current plays critical role in the welding arc force, which results in significant vibration in the molten pool. The higher pulse welding current facilitates the vibration in welding pool, consequently refine the grain size in weld. Meanwhile, the pulsed TIG welding can produce weld with lower heat input, which facilitates the refinement of the grain size for welding of nickel-based alloys. The grain refinement leads to the increase of hardness in the weld.

REFERENCES

[1] ASM Handbook, Volume 6: Welding, Brazing, and Soldering. 1993.

[2] John N. DuPont, John C. Lippold, and Samuel D. Kiser, Welding metallurgy and Weldability of nickel-base alloys, Wiley, a John Wiley & Sons, Inc., Publication, Hoboken, New Jersey. 2009.

[3] Nickel Development Institute, Guidelines for the welded fabrication of nickel alloys for corrosion-resistant service, Reference Book, Series No.: 11-012, 1994.

[4] Special Metals Corporation, Joining (Publication Number SMC-055), Huntington, WV, Oct. 2003.

[5] Myriam Brochu, Alexis Chiocca, Rafael Navalon-Cabanes, Jean Fournier, "Solidification Cracking of IN 718 TIG Welds", 13th International Conference on Fracture, Beijing, China, June 16–21, 2013.

[6] E. Farahani, M. Shamanian, F Ashrafizadeli, "A Comparative Study on Direct and Pulsed Current Gas Tungsten Arc Welding of Alloy 617", AMAE Int. J. on Manufacturing and Material Science, Vol. 02, No. 01, pp. 1 to 6, May 2012.

[7] John Norrish, Advanced welding processes, Woodhead Publishing Limited, Cambridge, England, 2006.

[8] https://www.millerwelds.com/resources/article-library/superior-for-stainless-highspeed-pulsed-gtaw-boosts-productivity-quality-while-reducing-distortion.

[9] D. W. Becker and C. M. Adams, Jr., "The Role of Pulsed GTA Welding Variables in Solidification and Grain Refinement", Welding Journal, pp. 143-s to 152-s, May 1979.

[10] ASME Boiler and Pressure Vessel Code, Section IX-Welding, Brazing, and Fusing Qualifications. 2019.

[11] M. L. Lin, and T. W. Eagar, "Pressures Produced by Gas Tungsten Arcs", Metallurgical Transactions B, Vol. 17B, pp. 601 to 607, Sep. 1986.

[12] John C. Lippold, Welding Metallurgy and Weldability, Wiley, 2014.